High-index dielectric metasurfaces performing mathematical operations

Andrea Cordaro[1,2], Hoyeong Kwon[3], Dimitrios Sounas[3,4], A. Femius Koenderink[2], Andrea Alù[3,5], and Albert Polman[2,*]

[1]Van der Waals-Zeeman Institute, Institute of Physics, University of Amsterdam Science Park 904, 1098 XH Amsterdam, The Netherlands
[2]Center for Nanophotonics, AMOLF Science Park 104, 1098 XG Amsterdam, The Netherlands
[3]Department of Electrical and Computer Engineering, The University of Texas at Austin, Austin, TX 78712, USA.
[4]Department of Electrical and Computer Engineering, Wayne State University, Detroit, MI 48202, USA
[5]Photonics Initiative, Advanced Science Research Center, City University of New York, New York, NY 10031, USA

We provide an intuitive explanation of our design strategy supporting it with Coupled Mode Theory and simulations. We explain the asymmetry requirements necessary to design metasurfaces performing odd-symmetry operations, such as 1st–order spatial differentiation. Next, we give a detailed description of the optical setups used to perform the measurements shown in the main text and an estimate of the metasurface's bandwidth of operation. Finally, we show the complete (real and imaginary part) calculated response of the metasurface compared to its ideal counterpart and an illustration of a possible practical implementation on an imaging system.

Design and Theory

The main idea behind our designs of metasurfaces for image processing is that their transfer function can be tuned by introducing a Fano resonance in transmission, and manipulating its dispersion asymmetry and linewidth. In order to prove this property, we use the general formula for a Fano lineshape[1,2]

$$|S_{21}| = \frac{(\varepsilon+q)^2}{\varepsilon^2+1} m, \tag{S1}$$

where S_{21} is the scattering matrix element representing transmission for a generic two-port optical system, $m = {}^{1}/_{(1+q^2)}$ is a normalization factor, and $\varepsilon(k_x) = {}^{2(\omega-\omega_0(k_x))}/_{\Gamma}$ is a dimensionless parameter that traces the detuning of the operation frequency ω relative to the resonance at $\omega_0(k_x)$ (dispersing with wavevector k_x), normalized to the linewidth Γ of the resonance. One way to achieve a dispersive resonance frequency is by using one of the leaky-wave resonances of the metasurface. In this case, incident waves are coupled to surface waves propagating along the metasurface through the additional momentum added to them by the metasurface and $\omega_0(k_x)$ generally follows the dispersion of these surface waves. The variable q is a phenomenological lineshape parameter which reflects the contribution of the discrete state in a Fano resonance relative to that of the continuum. Without specifying the nature of the resonance yet we show how it is possible to design the transfer function $|S_{21}(k_x)|$ by tuning the parameters in Eq.(S1). Starting with q, Figure S1a shows how it controls the asymmetry of the Fano lineshape: for $q = 0$ the transmission has a symmetrical dip at the reduced energy corresponding to the system resonance; for increasing values of q the lineshape evolves from a completely asymmetric one to a standard Lorentzian peak (for $q \to \infty$, data not shown). In the most general case, $\omega_0(k_x)$ can be expressed as $\omega_0(k_x) = \omega_0(0) + \sum_n \alpha_n (\frac{ck_x}{\omega_0(0)})^n$ by applying the Taylor expansion at $k_x = 0$. Note that k_x is normalized versus the free-space wavenumber at $\omega_0(0)$ so that all α_n are expressed in the same frequency units. In reciprocal structures $\omega_0(-k_x) = \omega_0(k_x)$, indicating that all the odd-order terms are zero ($\alpha_1 = \alpha_3 = \cdots = 0$). Then, the dominant term in the expansion is the one with $n = 2$, and in Figure S1b we plot the transmission as a function of the normalized frequency $\bar{\varepsilon} = {}^{2(\omega-\omega_0(0))}/_{\Gamma}$ and normalized wavenumber $\bar{k_x} = {}^{ck_x}/_{\omega_0(0)}$ for fixed values of q and Γ and assuming only the second-order dominant term in the Taylor expansion of $\omega_0(k_x)$ with $\alpha_2 = -{}^{3}/_{2}$. Taking a cross cut of the data at the $\bar{\varepsilon}$ of the minimum

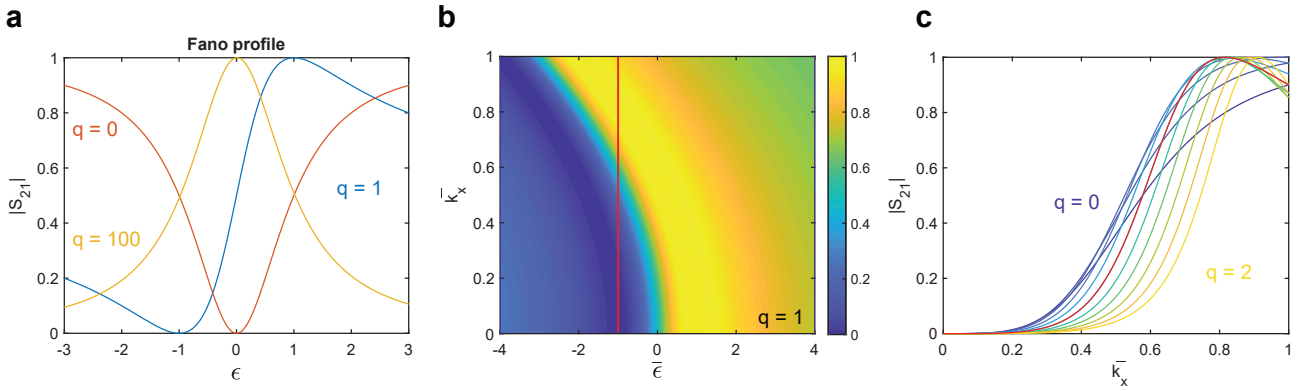

Figure S1. **a** Plot of $|S_{21}|$ (from Eq.(S1)) for $q = 0$ (orange solid line), $q = 1$ (blue solid line), $q = 100$ (yellow solid line). **b** Plot of $|S_{21}|$ (from Eq.(S1)) as function of $\bar{\varepsilon}$ and $\bar{k_x}$ for a parabolic dependence of ω_0 on k_x and fixed values for the shape parameter $q = 1$ and for the linewidth $\Gamma = 1$. **c** Plot of $|S_{21}|$ (from Eq.(S1)) as a function of $\bar{k_x}$ as q is changed from 0 (blue line) to 2 (yellow line) in steps of 0.2. The red solid line corresponds to the indicated cross-cut through b.

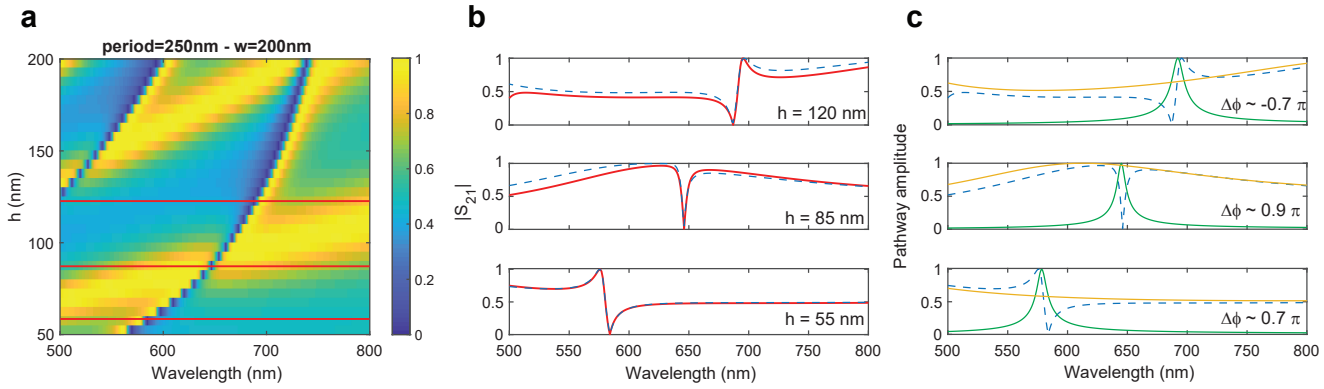

Figure S2. **a** Simulated transmission spectra of an array of nanobeams ($n = 4$, $w = 200$ nm, $p = 250$ nm) as the height h is swept from 50 nm to 200 nm. The electric field $\vec{\mathbf{E}}$ is polarized along the nanobeams.**b** Cross–cuts through a for $h = 55$ nm, $h = 85$ nm and $h = 120$ nm (red solid lines) and fitted spectra according to coupled-mode theory (blue dashed lines). **c** Amplitude of the direct (yellow) and resonant (green) pathways composing the fits (blue dashed lines).

for $k_x = 0$ it is possible to study the behavior of $|S_{21}(k_x)|$ as a function of q. As shown in Figure S1c, tuning the asymmetry of the Fano lineshape strongly affects the concavity and shape of the transfer function $|S_{21}(k_x)|$. In particular, for $q = 1$ a close-to-parabolic shape can be obtained, similar to what is desired for the optimized 2$^{\text{nd}}$–order differentiation. It is important that, in actual realizations, also q and Γ might disperse with k_x but for the sake of simplicity this is not taken into account here. Next, we discuss how the structural parameters of the metasurface are connected to the variables just described. While there is no trivial way to design $\omega_0(k_x)$, it is straightforward to tune q. Figure S2a shows the simulated transmission spectra of an array of nanobeams (refractive index $n = 4$) with fixed width ($w = 200$ nm) and periodicity ($p = 250$ nm) as the height h is swept from 50 nm to 200 nm. It easy to notice how the asymmetry of the Fano line shape changes as h is increased (see Figure S2b). The Fano lineshapes for this type of metasurfaces are induced by the interference between sharp quasi-guided modes that can be launched in-plane along the structure and a broader Fabry-Pérot (FP) background determined by the fill fraction F and the height h of the structure; these two different light pathways correspond to spectral features that are easily distinguishable in Figure S2a. Changing the height of the structure shifts the frequency response of both pathways

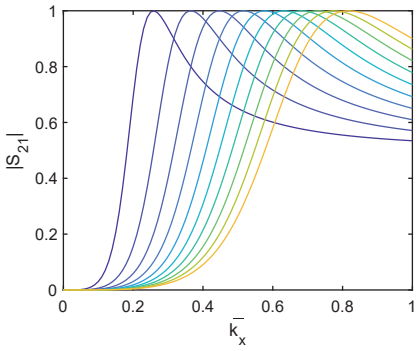

Figure S3. Plot of $|S_{21}|$ (from Eq.(S1)) as function of $\bar{k}_x$ for a parabolic dependence of ω_0 on k_x with $\alpha_2 = -3/2$ and a fixed shape parameter $q = 1$ as Γ is increased from 0.1 (blue line) to 1 (yellow line).

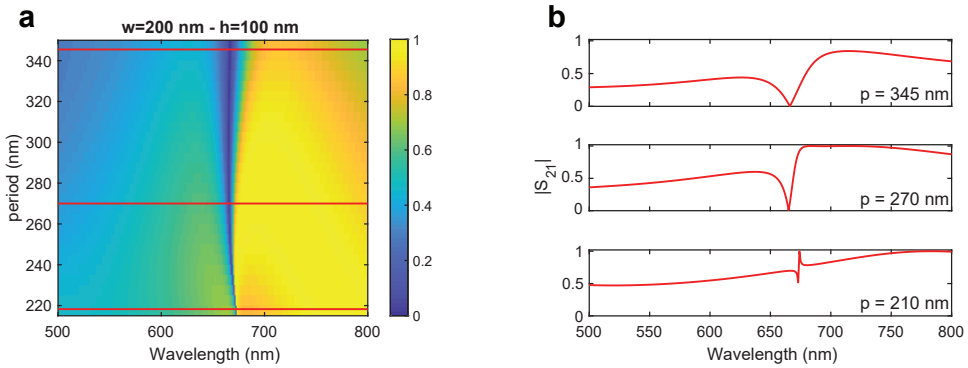

Figure S4. **a** Simulated transmission spectra of an array of nanobeams ($n = 4$, $w = 200$ nm, $h = 100$ nm) as the period p is swept from 205 nm to 350 nm. The electric field $\vec{\mathbf{E}}$ is polarized along the nanobeams. **b** Cross-cuts through a for $p = 210$ nm, $p = 270$ nm and $p = 345$ nm (red solid lines) .

and thereby controls the amplitude and phase at which they interfere to generate the asymmetric lineshape. This property is formalized in Coupled-Mode Theory (CMT) that provides an analytical form for the transmission of a system with a guided-mode resonance[3,4]

$$S_{21} = t \pm \frac{-(r \pm t)\gamma}{i(\omega - \omega_0) + \gamma}, \tag{S2}$$

where ω_0 is the resonance frequency, γ is the radiative leakage rate and r and t are the reflection and transmission Fresnel coefficient for a uniform slab of index $n_{\text{eff}} = [(1-F)n_0^2 + Fn^2]^{1/2}$ (with $n = 4$ and $n_0 = 1$)[5]. Thus, the first term in Eq.(S2) represents the broad FP background while the second term represents the guided-mode-resonant pathway. Since these two terms are complex valued it is important to study their phase difference $\Delta\phi = \arg(t) - \arg(\pm\frac{-(r\pm t)\gamma}{i(\omega-\omega_0)+\gamma})$ on resonance to understand how the two pathways combine and hence determine the final asymmetry of the Fano resonance. To do this, we fit the simulated transmission of Figure S2a for three different heights (see Figure S2b–c) using Eq.(S2). Figure S2c shows the amplitude of the two pathways that are composing the fitted functions (dashed blue lines) as well as their phase difference $\Delta\phi$ at the resonance wavelength (inset) highlighting the importance of this phase lag and its influence on the final resonant lineshape. To conclude, thickness tuning provides a direct handle on the asymmetry parameter in $|S_{21}|$, which in turn gives control over the curvature of the transfer function around $k_x = 0$.

Next, we assess how to control the numerical aperture of operation. This is directly controllable by the linewidth parameter Γ in Eq.(S1). Figure S3 shows $|S_{21}(k_x)|$ for fixed q and a parabolic $\omega_0(k_x)$ as Γ is increased. As the linewidth of the resonance is increased also the metasurface operational wavevector range is expanded. Hence, Γ

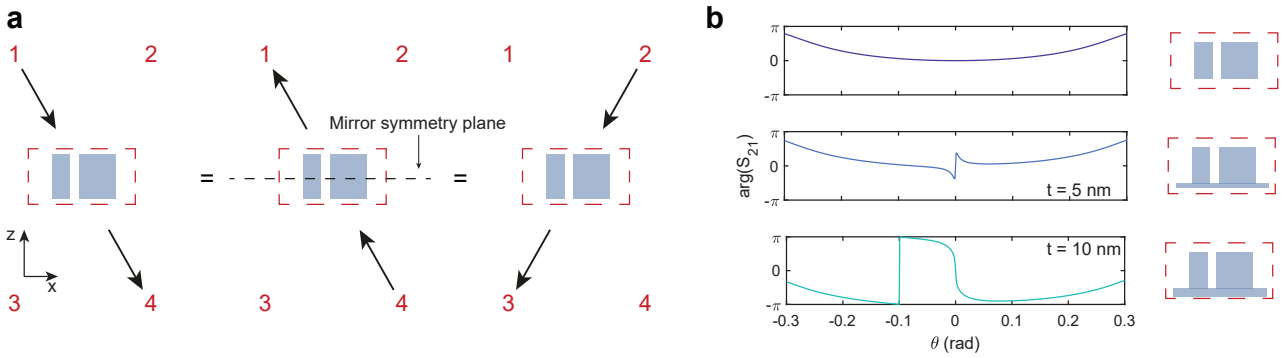

Figure S5. **a** The transmission response is still symmetric if only one of the symmetries is broken. **b** Simulated transmission phase of an array of nanobeams ($n = 4$, $w_1 = 40$ nm, $w_2 = 108$ nm, gap between the wires equal to 16 nm, $h = 100$ nm and $p = 250$) as the residual thickness t is increased from 0 to 10 nm. The electric field $\vec{\mathbf{E}}$ is polarized along the nanobeams.

allows direct tuning of the metasurface numerical aperture (NA). In simulation, it is possible to tune the linewidth by changing the array periodicity while keeping the nanobeam dimensions fixed, as shown in Figure S4a–b. However, an upper bound on periodicity is set by the opening of higher order diffraction channels at large pitches. These will complicate the design of the transfer function and drop the efficiency.

In the case of 1$^{\text{st}}$–order differentiation, not only the amplitude of the transfer function $|S_{21}(k_x)|$, but also the phase $\arg(S_{21}(k_x))$ is important. In fact, such operation requires a response that has odd–symmetry around the sample normal $S_{21}(-k_x) = -S_{21}(k_x)$. In other words, the transmission phase for positive k_x values should be phase-shifted by π compared to that of negative k_x values. In order to achieve this asymmetric phase response, it is necessary to break the unit cell's mirror symmetry both along the propagation (i.e. z–axis) and transverse (i.e. x–axis) directions. Invoking Lorentz reciprocity, it is easy to show that breaking the mirror symmetry only along the x–axis is not sufficient (see Figure S5a) to generate a transmission response of odd symmetry. Indeed, the transmission at negative incidence angles (from port 1 to 4) S_{41} has to be equal to the transmission from port 4 to 1, i.e. S_{14}, by reciprocity. Yet the latter has in turn to be equal to S_{32} if the symmetry along the z–axis is not also broken. Thus, at asymmetry along x yet mirror symmetry in z the transmission remains a symmetric function of k_x. This fact can also be observed in simulation as shown in Figure S5b. Adding a residual layer of thickness t below the nanobeams breaks the symmetry along the z–axis, and thereby provides the odd–symmetry system response required for odd–order differentiation. Simulations show that the thickness t provides control over the phase asymmetry (see Figure S5b).

Experiment

In order to assess the processing capabilities of the metasurfaces, an image is projected onto the sample and the outcome is inspected on a CCD camera using the optical setup in Figure S6. The illumination is provided by a SuperK EXTREME/FIANIUM supercontinuum white light laser that is monochromated (1 nm bandwidth) by an Acousto-Optic Tunable Filter (AOTF) and subsequently coupled to a single mode fiber. The output of the fiber is collimated by a condenser lens and passed through a spinning diffuser plate to evenly illuminate the image which is composed of Cr patterns on glass. The diffuser also serves to remove speckle artefacts in imaging that otherwise occur due to the large spatial coherence of the source. The image is projected at unit magnification onto the metasurface by two Olympus MPlanFL N 20x-0.45NA objectives. The second half of the setup is a standard microscope with Fourier imaging capabilities, already reported in Ref.[6]: the image is collected by either of two objectives (Nikon Plan Fluor 20X – 0.5NA and Nikon S Plan Fluor ELWD 60X – 0.7NA) and projected onto a Photometrics CoolSNAP EZ silicon CCD camera by a 20 cm focal distance tube lens. In between objective and tube lens, a 1:1 telescope provides an intermediate real space plane, while flipping in the Fourier (or Bertrand) lens allows projection of the back focal plane of the objective directly onto the CCD[7] (Fourier imaging mode, unit magnification

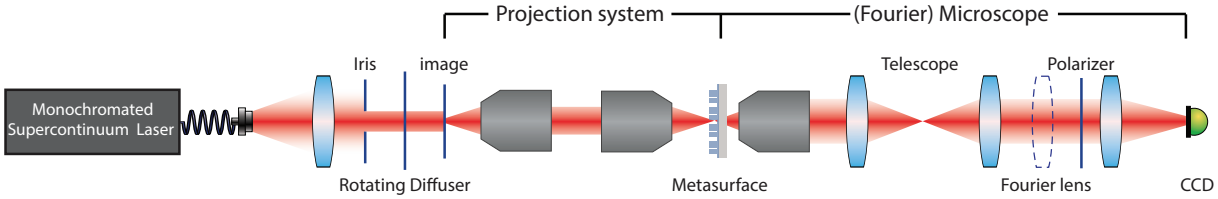

Figure S6. The setup consist of a projection system coupled to a standard microscope with Fourier imaging capabilities.

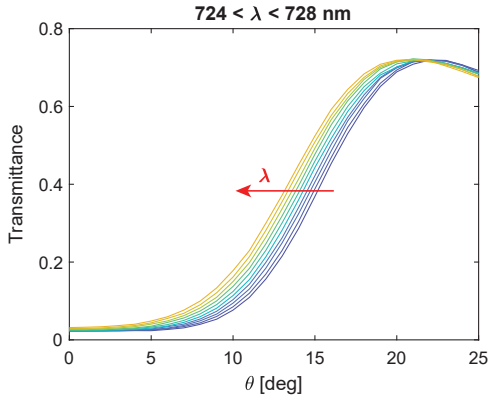

Figure S7. Measured transmittance as function of incident angle for different wavelengths in the range 724–728 nm. Experimental data from Figure 4a of the main text.

from back focal plane to objective). In order to collect the data shown in the inset of Figure 4b of the main text, the first objective (from left) is removed and the Fourier lens is flipped in.

The data in Figure 4a of the main text were collected with a Spectra Pro 2300i spectrometer equipped with a Pixis 400 CCD. The sample was mounted on a rotating stage and illuminated with collimated white light from a SuperK EXTREME/FIANIUM supercontinuum laser. The transmitted light was collected by an integrating sphere and sent to the spectrometer through a multimode fiber. For both setups, light is polarized along the nanobeams direction. Using the same dataset of Figure 4a of the main text, it is possible to give an estimate of the bandwidth of operation. The designed Fano resonances have a relatively low Q factor ($Q \simeq 24$) hence the bandwidth of operation is relatively large and achievable with filtered white light. As shown in Figure S7, the shape of the transfer function does not change significantly as the illumination wavelength is varied over a bandwidth of 4 nm around the optimum.

Supplementary figures

In order to elucidate the performance of our designs we compare the metasurface response with its ideal counterpart in Figure S8. It is easy to notice that the metasurface output is very close to the ideal one both in real and imaginary part. The transfer functions used for the metasurface outputs are the same as in Figure 2a-d of the main text. Regarding the ideal differentiation, $T_1 = ik_x$ and $T_2 = -k_x^2$ were used as transfer functions for 1^{st}– and 2^{nd}–order derivative respectively. In conclusion, the performance of the metasurface may be already amenable for augmented reality applications operating around a specific wavelength. Furthermore, we note that multiple metasurfaces may be designed to operate at different wavelengths to match the RGB color filters of a standard CCD. It is important to stress that this is possible because the metasurface operates in the image plane, and not in the Fourier plane of the projected image, as shown in Figure S9.

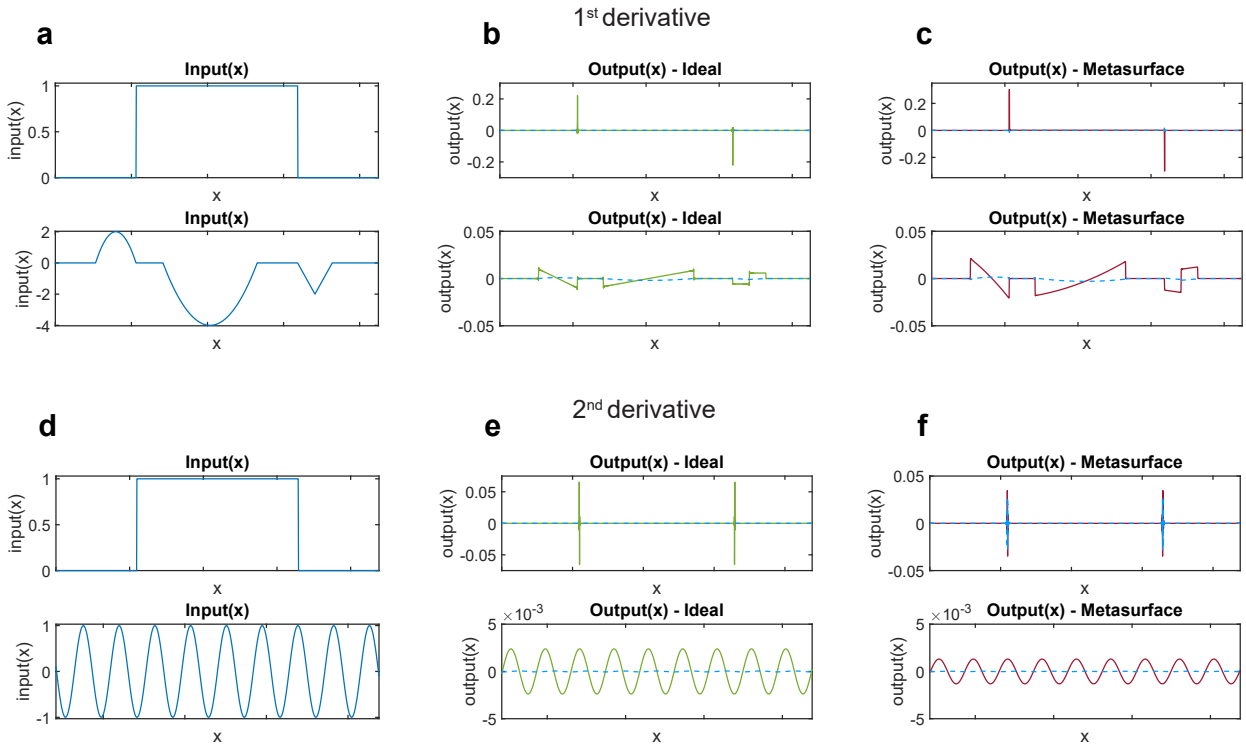

Figure S8. Metasurfaces performing 1st– and 2nd–order spatial differentiation. **a-d** Input functions used to numerically test the metasurface operation. The signal is discretized into 2048 pixels with individual pixel size set such that the Nyquist range matches the operational range in k-space of the metasurface. **b-e** Ideal output for the input in a-d. **c-f** Metasurface output for the input in **a-d**. The solid line represents the real part while the dashed line represents imaginary part of the output.

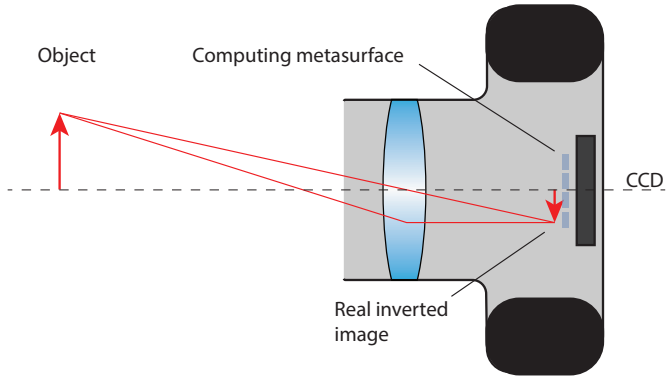

Figure S9. Illustration of a possible practical metasurface implementation on an imaging system. The metasurface performing the derivative operation on the image is placed directly onto the CCD of a standard camera.

References

1. Fano, U. Sullo spettro di assorbimento dei gas nobili presso il limite dello spettro d'arco. *Il Nuovo Cimento* **12**, 154–161 (1935).

2. Miroshnichenko, A. E., Flach, S. & Kivshar, Y. S. Fano resonances in nanoscale structures. *Rev. Mod. Phys.* **82**, 2257–2298 (2010).

3. Fan, S., Suh, W. & Joannopoulos, J. D. Temporal coupled-mode theory for the Fano resonance in optical resonators. *J. Opt. Soc. Am. A* **20**, 569–572 (2003).

4. Haus, H. A. *Waves and fields in optoelectronics* (Prentice-Hall, Englewood Cliffs, N.J, 1984).

5. Brundrett, D. L., Glytsis, E. N. & Gaylord, T. K. Homogeneous layer models for high-spatial-frequency dielectric surface-relief gratings: conical diffraction and antireflection designs. *Appl. Opt.* **33**, 2695 (1994).

6. Sersic, I., Tuambilangana, C. & Femius Koenderink, A. Fourier microscopy of single plasmonic scatterers. *New J. Phys.* **13**, 083019 (2011).

7. Kurvits, J. A., Jiang, M. & Zia, R. Comparative analysis of imaging configurations and objectives for Fourier microscopy. *J. Opt. Soc. Am. A* **32**, 2082 (2015).